Envelope and waveguide methods: a comparative study of PbF_2 and CeO_2 birefringent films

F. Horowitz and S. B. Mendes

We have characterized low-birefringence, PbF_2 coatings to permit, first, agreement between envelope and prism-coupler waveguide methods under the standard isotropic assumption. In essentially the same measurement conditions, for obliquely deposited (58.3°) CeO_2 coatings the isotropic model becomes unsustainable. Explicit consideration of the film microstructure is then required for good correlation between thickness results from TE (503 ± 9 nm) and TM (504 ± 10 nm) modes in the waveguide experiment as well as between refractive-index results from envelope (n_2 = 1.78 ± 0.03) and waveguide (n_2 = 1.794 ± 0.002) techniques. We considered uniaxial and biaxial models to achieve consistency, and the refractive indices along the principal axes of symmetry were determined.

Key words: Thin films, birefringence, characterization.

Introduction

Knowledge of the optical constants of a thin film is today a key element in the improvement of optical components based on coating technology. The challenge of high optical quality under tight tolerances, through advances that have occurred over the last few decades on deposition parameter control and design techniques for multilayer interference filters, has shifted to a better understanding of the optical properties of materials in film form.[1]

In this respect limited correlation has been found among the results from different characterization methods. Significant discrepancies in the refractive-index measurements of Sc_2O_3 films were shown a few years ago in a joint project by seven prominent laboratories.[2] That research has confirmed the need for models of film microstructure that depart from the standard homogeneity and isotropy assumptions, as already indicated by earlier reports on electron microfractography,[3] computer simulation,[4] and light scattering.[5]

In a previous investigation[6] Macleod and Horowitz considered a columnar microstructure model to interpret a combination of ellipsometry and Abelès techniques. That investigation allowed for the unambiguous characterization of ZrO_2 films, which were thermally deposited at 65° vapor incidence.

From the same perspective, in this paper we aim at understanding the influence of the anisotropic microstructure of thin films on their optical properties, as shown by the envelope and waveguide methods.

This pair of methods is particularly interesting because it provides conditions for the material structure to be investigated by light from different angles. In the envelope method the transmittance spectrum is obtained after light traverses the film at normal incidence. In the waveguide method the synchronous angles, each corresponding to one guided mode, are measured after light propagates along the film.

Theoretical Background

Prism-Coupler Waveguide Method

For an isotropic waveguide with index of refraction n, surrounded by two parallel interfaces labeled a and b as in Fig. 1, the well-known[7] mode equation applies:

$$\frac{2\pi}{\lambda} d\beta^f = \theta_a + \theta_b + m\pi, \quad (1)$$

where β^f is the propagation parameter defined as

$$\beta^f \equiv (n^2 - v^2)^{1/2}, \quad (2)$$

The authors are with the Instituto de Física, Universidade Federal de Rio Grande do Sul, Campus do Vale, Caixa Postal 15051, 91500 Porto Alegre, Rio Grande do Sul, Brazil.

Received 7 July 1992; revised manuscript received 23 August 1993.

0003-6935/94/132659-05$06.00/0.

where $v \equiv (ck_x/w)$ and

$$\text{s polarization} \qquad \text{p polarization}$$

$$\tan(\theta_i) \equiv \frac{\beta^i}{\eta_s}, \qquad \tan(\theta_i) \equiv \frac{\eta_p \beta^i}{{n_i}^2}, \tag{3}$$

$$\eta_s \equiv (n^2 - v^2)^{1/2}, \qquad \eta_p \equiv \frac{n^2}{(n^2 - v^2)^{1/2}}, \tag{4}$$

$$\beta^i \equiv (v^2 - {n_i}^2)^{1/2}, \qquad i = a, b. \tag{5}$$

When the waveguide material is anisotropic, provided one of its principal axes of symmetry is orthogonal to the plane of incidence (i.e., in the *s*-polarization direction), Eq. (1) remains valid. This validity has been rigorously shown through a 4 × 4 matrix formalism for both uniaxial[8] and biaxial[9] cases. In such a condition the *s*- and *p*-polarization modes are uncoupled, and thus they can be treated as propagating independently in the waveguide. The equations above can still be used, except for Eqs. (2) and (4), which are replaced by[9]

$$\beta_s{}^f \equiv ({n_2}^2 - v^2)^{1/2},$$

$$\beta_p{}^f \equiv \frac{n_1 n_3 [{n_1}^2 \sin^2(\phi) + {n_3}^2 \cos^2(\phi) - v^2]^{1/2}}{{n_1}^2 \sin^2(\phi) + {n_3}^2 \cos^2(\phi)}, \tag{6}$$

$$\eta_s \equiv ({n_2}^2 - v^2)^{1/2},$$

$$\eta_p \equiv \frac{n_1 n_3}{[{n_1}^2 \sin^2(\phi) + {n_3}^2 \cos^2(\phi) - v^2]^{1/2}}, \tag{7}$$

where conventions used for the principal refractive indices are as in Fig. 1.

Envelope Method

With the conventions of Fig. 2 incoherent summation over multiple reflections at both substrate interfaces leads to the overall transmissivity at normal incidence:

$$T = \frac{T_1 T_s}{1 - R_2 R_s}, \tag{8}$$

where R_s and T_s refer to the substrate–air interface and T_1 and R_2 refer to the air–film–substrate subsystem, which are determined by use of a coherent treatment and Fresnel relations, so that in the weak absorption regime Eq. (8) becomes

$$T \cong \frac{A_1' x}{A_2' - A_3' x \cos(2\gamma) + A_4' x^2}, \qquad x \equiv \exp(-2\alpha) \tag{9}$$

as in Swanepoel,[10] where phase thickness $\gamma = 2\pi n d/\lambda$, absorption coefficient $\alpha = 2\pi k d/\lambda$, and the A' coefficients are explicit functions of the real refractive indices of the media involved.

For a high-index film with $n > n_s$, for example, T_{max} or T_{min} envelope curves are obtained from Eq. (9) with $\cos(2\gamma)$, assuming values of +1 or −1, respectively. These values correspond to the following spectrum positions:

$$\lambda = \frac{4nd}{2m} \quad \text{for } T = T_{max} \tag{10}$$

or

$$\lambda = \frac{4nd}{2m + 1} \quad \text{for } T = T_{min}. \tag{11}$$

Through a combination of T_{max} and T_{min} so that x is eliminated, the real part of the film refractive index is given by

$$n = [N \pm (N^2 - {n_o}^2 {n_s}^2)^{1/2}]^{1/2}, \tag{12}$$

with

$$N \equiv 2 n_o n_s \left(\frac{1}{T_{min}} - \frac{1}{T_{max}}\right) + \frac{{n_o}^2 + {n_s}^2}{2}.$$

If n is known, d is determined by use of at least any two identities, Eq. (10) or (11), so that m is eliminated. From n and d, m is immediately found. Furthermore, one can iteratively refine n and d results through the Swanepoel[10] procedure by imposing on the interference order m an integer value that is the closest to that previously calculated.

In the anisotropic case, provided the incident polarization is taken as along or orthogonal to one of the principal axis of symmetry, those two components

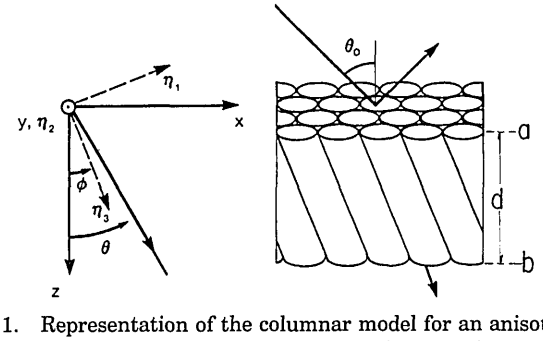

Fig. 1. Representation of the columnar model for an anisotropic film with the principal indices shown along the axes of symmetry.[6] η_1–η_3, symmetry; x, y, z, ϕ, and θ, coordinate variables.

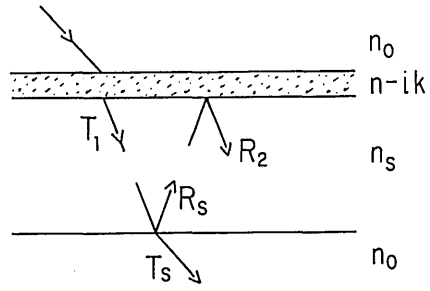

Fig. 2. Thin film deposited on a transparent substrate surrounded by air with the conventions shown for the envelope method calculations.

traverse the film uncoupled, and therefore they can be treated independently in the above manner. When we refer to Fig. 1 and Eq. (12) the effective refractive indices obtained by this method are related to the principal refractive indices, as in Eq. (7) with $\alpha = 0$, through the equations

$$n_{\parallel} = n_2, \tag{13}$$

$$n_{\perp} = \frac{n_1 n_3}{[n_1^2 \sin^2(\phi) + n_3^2 \cos^2(\phi)]^{1/2}}, \tag{14}$$

which correspond to an incident polarization parallel and perpendicular to the second principal axis of symmetry, respectively.

Experimental Procedure

For the envelope method we measured normal-incidence transmission spectra in the visible and near IR from a Cary 14 spectrophotometer updated with a latest universal spectrophotometer interface (LUSI) attachment. The procedure was normal, except for the following two additional steps.

The films deposited at high angles of vapor incidence presented pronounced thickness nonuniformity. For that reason[11] the spectrophotometer beam aperture was reduced until no attenuation of contrast in transmittance spectrum could be seen. The diameter of the aperture was in the 1–2-mm range, and the cone angle of the light beam was in the 2–3-deg range.

An HN-32 Polaroid was inserted into the sample beam trajectory and rotated 90° to provide polarizations parallel and perpendicular to one of the principal axes of the film microstructure. That choice was made, in opposition to a sample rotation, so that the illuminated spot on the sample would remain unchanged throughout the measurement.

In the waveguide experiment the main Otto[12] configuration was used, as shown in Fig. 3. However, the prism coupler was a hemisphere made of Schott SF-11 optical glass with refractive index $n_h = 1.77862$ at the He–Ne laser wavelength. It was supported by a $\theta - \varphi$ positioner over an X–Y translator. The Zeiss-Jena goniometer could provide reading precisions of better than 0.5 arcmin.

We refined the standard alignment procedures further by observing Newton rings in backreflectance conditions. In addition we minimized the influence of residual instrument and alignment errors by an exhaustive number of measurements (~ 30) of each synchronous angle, redundantly taken at both sides of the hemisphere.

Films for this study were thermally deposited on clean transparent glass in a vacuum chamber with ground pressures of 10^{-6} mbars. Resistive heating of a W boat was employed for the PbF_2 films, while the CeO_2 films were reactively deposited from Mo boats in an O_2 atmosphere at typical working pressures of 10^{-4} mbars. Deposition geometry was carefully controlled in each run, with particular attention to the vapor angle of incidence.

Results and Discussion

Weak Anisotropy Regime

To check for consistency between the waveguide and spectrophotometer experimental results, PbF_2 films were deposited at normal vapor incidence. Data from the waveguide method are shown in Fig. 4.

The refractive-index values obtained for the films are close to that of bulk PbF_2, which indicates that reasonably high packing densities were achieved. Furthermore Fig. 4 indicates that the isotropic model, although pores are present in the film, performs well enough to provide a spread of refractive index and thickness values within the experimental uncertainties.

Another set of measurements, after the sample was rotated by an azimuthal angle of 90°, produced practically the same refractive-index results as in Fig. 4 with the TE and TM values interchanged, which indicates not only consistency within the waveguide method but also negligible sensitivity to small angular variations in sample orientation. Thickness variations, however, were slightly higher than experimental uncertainties, which reveals sample nonuniformity under small shifts in position.

With those considerations in mind and from a spectrophotometer transmission scan, we compared refractive-index values obtained through the envelope method with those from the waveguide experiment in Fig. 5.

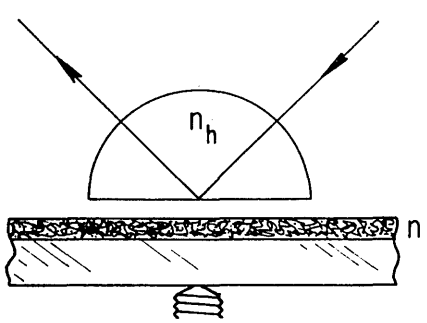

Fig. 3. Configuration of the waveguide experiment with the hemispherical coupler.

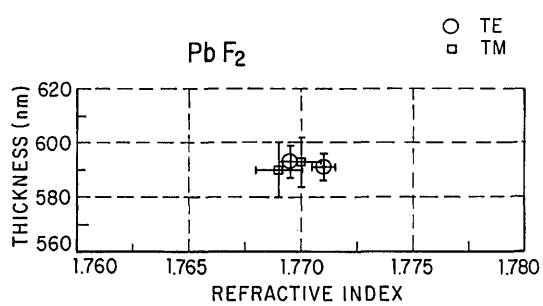

Fig. 4. Thickness versus refractive index for a normally deposited PbF_2 film as seen by the waveguide method. The two TE–TM pairs refer to the left and right sides of the hemispheric prism coupler.

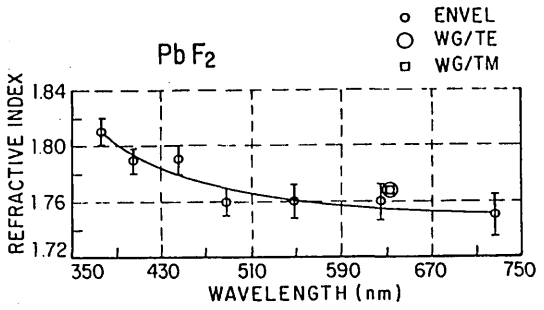

Fig. 5. Refractive-index data from the envelope and waveguide methods for a PbF_2 film thermally deposited at normal vapor incidence.

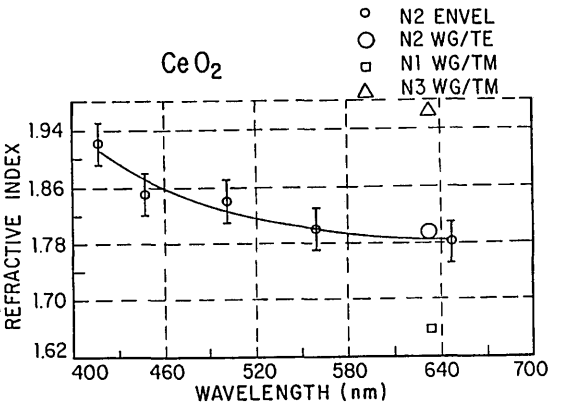

Fig. 7. Refractive-index data of a CeO_2 film from envelope and waveguide (WG) TE and TM measurements. The film was deposited at 58.3°, and a biaxial model with $n_2 \equiv n^{TE}$ was considered.

Strong Anisotropy Regime

Once we obtained good consistency between the two experimental settings in weak anisotropy conditions, films of CeO_2 with a high bulk refractive index were deposited at oblique vapor incidence to enhance anisotropic behavior. For a typical sample, on which repeated measurements were taken, a vapor angle of 58.3° by the tangent rule[13] implied a columnar angle of 39.0°, both with respect to the surface normal.

Even when we start from an isotropic model, significant refractive-index differences Δn between the TE and TM modes resulted. Right (R) and left (L) typical data are presented in Fig. 6 as well as mean standard deviations σ that represent the remaining uncertainties after a large number of measurements. Relative values are $(\Delta n/\sigma)_R \geq 20$ and $(\Delta n/\sigma)_L \geq 56$.

The thickness values are not in satisfactory agreement even when measurement imprecisions are considered.

The whole picture illustrates the need for models that take into account explicitly the anisotropic microstructure. Moreover careful analysis of the theory shows that an equivalent isotropic index can be taken for the TE polarization along one of the principal axes of symmetry but that a similar association is incorrect for the TM polarization.[9]

In the next step we consider a uniaxial model by assuming that $n_1 = n_2$, whose results are also shown in Fig. 6. Now the birefringence is even more pronounced with $(\Delta n)_R = 0.098 \pm 0.007$ and $(\Delta n)_L = 0.093 \pm 0.004$, whereas the thickness data come close to an agreement within experimental uncertainties, as indicated by the error bars in Fig. 6.

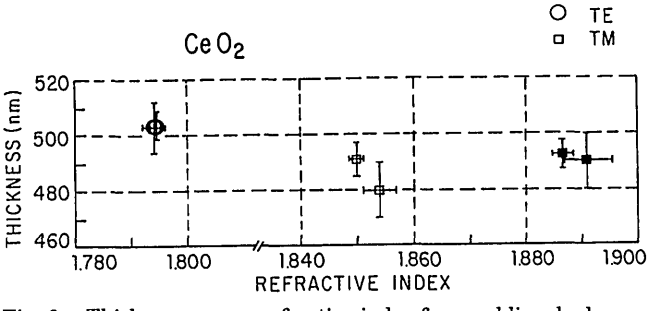

Fig. 6. Thickness versus refractive index for an obliquely deposited CeO_2 film as seen by isotropic (□) and uniaxial (■) models. The TE (○) results from both cases are coincident.

For the more general and accurate biaxial columnar model, since the CeO_2 film would guide only two TM modes, an additional measurement by the envelope method was performed. Here the TE polarization is still set along one of the principal axes of symmetry, so that $n_{TE} = n_2$.

The consistency between the two experiments was at first confirmed by the good agreement between $n_2^{EN} = 1.78 \pm 0.03$ (envelope method) and $n_2^{WG} = 1.794 \pm 0.002$ (waveguide method) at 632.8 nm, as represented in Fig. 7.

To determine n_1 and n_3 we used a combination of Eqs. (3), (6), and (7) for the TM mode in the waveguide method and Eq. (14) for the envelope method. Details are described in Ref. 9. As a final confirmation, good agreement in thickness values was obtained from both TE and TM results: $d^{TE} = (503 \pm 9)$ nm and $d^{TM} = (504 \pm 10)$ nm, where average values and the highest mean deviation errors were taken from left- and right-side measurements.

Conclusion

The consistency between envelope and waveguide methods was first established with PbF_2 films in weak anisotropy conditions, where the isotropic assumption remained as a reasonable approximation.

In the strong anisotropy regime, however, the microstructure has to be taken into account explicitly, which leads to more general expressions for both characterization methods. Here we consider those expressions for uniaxial and biaxial structures, provided a proper sample orientation is chosen to assure uncoupled propagation of linearly polarized modes. This choice permits the expressions to retain most of the simplicity of their isotropic counterparts and is applicable to practically all single-film experimental settings [see Eqs. (1), (2), (7), (12), (13), and (14)].

Such understanding permits unambiguous determination of thickness and refractive-index values of strongly anisotropic films, with consistency well within experimental errors from the envelope and waveguide

methods. This approach was illustrated for a CeO_2 film thermally deposited at 58.3 deg, for which thickness $d = 503 \pm 9$ nm, $n_1 = 1.65 \pm 0.05$, $n_2 = 1.794 \pm 0.002$, and $n_3 = 1.97 \pm 0.06$. The columnar model, with its correspondent principal axes of symmetry, then arises as a framework for a fundamental set of refractive indices into which measurement results from different techniques can be translated.

Even when undesirable, birefringence can be measured to monitor film packing densities in ion plating or other ion-assisted deposition processes.[14] Although anisotropy in this study is restricted to vacuum thermally deposited coatings, the procedure is essentially the same for films that consist of other birefringent materials, such as polymers and solid or liquid crystals.

Most results presented here are part of the thesis of Sergio Brito Mendes for the graduate program at the Physics Institute at the Brazilian Federal University of Rio Grande do Sul. He is currently at the Optical Sciences Center, University of Arizona, Tucson, Ariz. 85721; Michael R. Jacobson from there helped us obtain the spectrophotometer employed in the above measurements. We are also grateful to the Conselho Nacional de Pesquisas, the Fundação de Amparo a Pesquisa no Rio Grande do Sul, and the Programa de Apoio ao Desenvolvimento Científico e Tecnológico for partial support as well as to Wanda A. Knebel for typing and editing the final text.

References

1. H. A. Macleod, "The microstructure of optical thin films," in *Optical Thin Films,* R. I. Siddon, ed., Proc. Soc. Photo-Opt. Instrum. Eng. **325,** 21–28 (1982).
2. D. P. Arndt, R. M. A. Azzam, J. B. Bennett, J. P. Borgogno, C. K. Carniglia, W. E. Case, J. A. Dobrowolski, U. J. Gibson, T. Tuttle Hart, F. C. Ho, V. A. Hodgkin, W. P. Klapp, H. A. Macleod, E. Pelletier, M. K. Purvis, D. M. Quinn, D. H. Strome, R. Swenson, P. A. Temple, and T. F. Thonn, "Multiple determination of the optical constants of thin-film coating materials," Appl. Opt. **23,** 3571–3596 (1984).
3. J. M. Nieuwenhiuzen and H. B. Haanstra, "Microfractography of thin films," Philips Tech. Rev. **27,** 87–91 (1966).
4. M. Sikkens, I. J. Hodgkinson, F. Horowitz, H. A. Macleod, and J. J. Wharton, "Computer simulation of thin film growth: applying the results to optical coatings," Opt. Eng. **25,** 142–147 (1986).
5. F. Horowitz and H. A. Macleod, "Form birefringence in thin films," in *Los Alamos Conference on Optics '83,* R. S. McDowell and S. C. Stotlai, eds., Proc. Soc. Photo-Opt. Instrum. Eng. **380,** 83–87 (1983).
6. F. Horowitz and H. A. Macleod, "Determination of principal refractive indices of birefringent films," in *Optical Interference Coatings,* Vol. 6 of 1988 OSA Technical Digest Series (Optical Society of America, Washington, D.C., 1988), pp. 203–206.
7. P. K. Tien, "Light waves in thin films and integrated optics," Appl. Opt. **10,** 2395–2413 (1971).
8. M. O. Vassel, "Structure of optical guided modes in planar multilayers of optically anisotropic materials," J. Opt. Soc. Am. **64,** 166–173 (1974).
9. S. B. Mendes, "Comparative analysis of envelope and waveguide methods with extension to anisotropic microstructures in dielectric films," M.Sc. thesis (Instituto de Física, Universidade Federal do Rio Grande do Sul, Brazil, 1991).
10. R. Swanepoel, "Determination of the thickness and optical constants of amorphous silicon," J. Phys. E **16,** 1214–1222 (1983).
11. R. Swanepoel, "Determination of surface roughness and optical constants of amorphous silicon," J. Phys. E **17,** 896–903 (1984).
12. A. Otto, "Excitation of nonradiative surface plasma waves in silver by the method of frustrated total reflection," Z. Phys. **216,** 399–410 (1968).
13. A. G. Dirks and H. J. Leamy, "Columnar microstructure in vapor-deposited thin films," Thin Solid Films **47,** 219–233 (1977).
14. H. A. Macleod, Optical Science Center, University of Arizona, Tucson, Ariz. 85721 (personal communication, 1988).